Supporting Information

Lighting with organophosphorus materials: solution-processed blue/cyan light-emitting devices based on phosphaphenalenes

Philip Hindenberg,[a] Johannes Zimmermann,[b,e] Gerardo Hernandez-Sosa,[b,c,e] and Carlos Romero-Nieto*[a,c,d]*

E-mail: gerardo.sosa@kit.edu; carlos.romero.nieto@oci.uni-heidelberg.de

[a]Organisch-Chemisches Institut, Ruprecht-Karls-Universität Heidelberg, Im Neuenheimer Feld 270, 69120 Heidelberg, Germany. E-mail: carlos.romero.nieto@oci.uni-heidelberg.de

[b]Light Technology Institute, Karlsruhe Institute of Technology, Engesserstr. 13, 76131 Karlsruhe, Germany. E-mail: gerardo.sosa@kit.edu

[c]HEiKA – Heidelberg-Karlsruhe Research Partnership, University of Heidelberg, Karlsruhe Institute of Technology, Heidelberg, Germany

[d]Faculty of Pharmacy, University of Castilla-La Mancha, Calle Almansa 14 – Edif. Bioincubadora, 02008 Albacete, Spain

[e]InnovationLab, Speyerer Str. 4, 69115 Heidelberg, Germany

Table of Contents:

1. General section:

Reactions were carried out in dry glassware and under inert atmosphere of purified argon or nitrogen using Schlenk techniques. All solvents (diethyl ether, CH_2Cl_2, THF) were used directly from a solvent purification system MB SPS-800. P,P-dichlorophenyl phosphine, 1,8-dibromonaphthalene and 1-methyl-2-(4,4,5,5-tetramethyl-1,3,2-dioxaborolan-2-yl)-1*H*-indole were purchased from commercial suppliers and used as received. Compound **1** was prepared according to a reported procedure.[S1]

NMR: ^1H, ^{13}C and ^{31}P NMR as well as COSY and ROESY spectra were recorded on a Bruker Avance III, Bruker Avance 400, Bruker Avance-III-300, Bruker Avance DRX-300, Bruker Avance 500 or Bruker Avance 600. Chemical shifts are expressed as parts per million (ppm, δ) and referenced to external 85% H_3PO_4 (^{31}P), or solvent signals (^1H / ^{13}C): $CDCl_3$ (7.27 / 77.16 ppm) and CD_2Cl_2 (5.33 / 53.80 ppm) as internal standards. Signal descriptions include: s = singlet, d = doublet, t = triplet, m = multiplet and br = broad. All coupling constants are absolute values and *J* values are expressed in Hertz (Hz).

Mass spectrometry: MS and HRMS were measured at the Institute of Organic Chemistry at the University of Heidelberg. JEOL AccuTOF GCx time-of-flight for EI+ and Bruker ApexQe hybrid 9.4T FT-ICR for DART. GCMS was performed in a GC system 7890a from Agilent Technologies.

Theoretical calculations: Theoretical calculations have been carried out at the B3LYP/6-31+G(d) level of theory by using the GAUSSIAN 03 suite of programs.[S2] The calculations of compound **1** were repeated for this work; the results are in agreement with previously reported results.[S1] TD-DFT calculations were carried out at the B3LYP/6-31+G(d) level of theory using dichloromethane as solvent.

Electrochemistry: Voltammograms (cyclic voltammetry, differential pulse voltammetry and square wave voltammetry) were recorded using a Metrohm Autolab PGSTAT101 potentiostat/galvanostat from acetonitrile solutions using tetrabutylammonium hexafluorophosphate as electrolyte, glassy carbon as working electrode, Pt wire as counter electrode and Ag wire as pseudo-reference electrode. Scan rate is 100 mV s^{-1}. The curves were calibrated using ferrocene as internal standard ($E_{1/2}$ = 0.54 V vs SCE).

OLED Fabrication: Both emitter materials were spin coated from solution onto PEDOT-coated ITO-glass. Material **1** was dissolved at 5g/l in toluene, while material **2** in ethanol at 5g/l. After spin coating TPBi was evaporated to improve the device electron transport properties and charge injection. Followed by two final evaporation steps to fabricate a LiF/Al top electrode. The whole fabrication process took place under inert atmosphere.

Electrofluorochromic devices: The material dissolved in acetonitrile and tetrabutylammonium hexafluorophosphate was sandwiched between two ITO electrodes. The devices were biased using a Keithley 2400 voltage source and the spectral changes recorded with a UV-Vis spectrometer.

2. Synthetic procedures

2-(8-Bromonaphthalen-1-yl)-1-methyl-1*H*-indole C

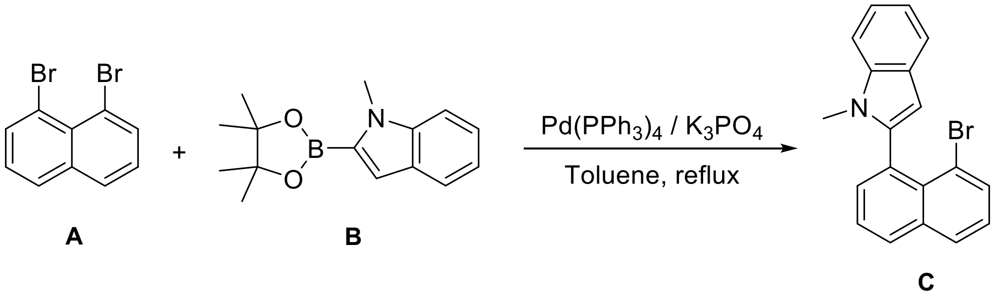

Scheme S1. Synthetic scheme for the preparation of the 2-(8-Bromonaphthalen-1-yl)-1-methyl-1H-indole

1-Methyl-2-(4,4,5,5-tetramethyl-1,3,2-dioxaborolan-2-yl)-1*H*-indole (1 eq, 1.75 mmol, 450 mg), 1,8-dibromonaphthalene (1 eq, 1.75 mmol, 500 mg), Pd(PPh$_3$)$_4$ (3 mol%, 52.5 µmol, 61 mg) and K$_3$PO$_4$ (3 eq, 5.25 mmol, 1.11 g) were suspended in 160 mL of toluene and the mixture was stirred at 130 °C. After 2 days, additional 1-methyl-2-(4,4,5,5-tetramethyl-1,3,2-dioxaborolan-2-yl)-1*H*-indole (0.25 eq, 437 µmol, 112 mg) was added and the mixture was stirred again at 130 °C for 2 days. The crude was allowed to reach room temperature and the crude mixture was quenched with 50 mL of H$_2$O, diluted with toluene and neutralized with 2M HCl aqueous solution. The aqueous phase was extracted with toluene and the combined organic phases were washed with H$_2$O and brine. After drying over MgSO$_4$, the solvent was removed under reduced pressure. The crude was taken up in toluene and purified by column chromatography, using alumina and pentane/toluene as an eluent mixture (9:1, progressively increasing the polarity to 8:2). 156 mg of a colorless solid were obtained (Yield: 27%). **^{1}H NMR** (600 MHz, in CDCl$_3$): δ 8.00 (d, *J* = 8.0 Hz, 1H), 7.94 (d, *J* = 8.3 Hz, 1H), 7.85 (d, *J* = 7.2 Hz, 1H), 7.69 (d, *J* = 8.0 Hz, 1H), 7.62 (dd, *J* = 6.9, 1.1 Hz, 1H), 7.57 (t, *J* = 7.6 Hz, 1H), 7.39 (d, *J* = 8.1 Hz, 1H), 7.34 (t, *J* = 7.7 Hz, 1H), 7.29 – 7.26 (m, 1H), 7.19 (t, *J* = 7.5 Hz, 1H), 6.57 (s, 1H), 3.40 (s, 3H). **^{13}C{^{1}H} NMR** (151 MHz, in CDCl$_3$): δ 140.2 (s, C), 136.8 (s, C), 135.8 (s, C), 134.1 (s, CH), 133.2 (s, CH), 131.0 (s, C), 130.8 (s, CH), 130.1 (s, C), 129.2 (s, CH), 128.4 (s, C), 126.4 (s, CH), 125.5 (s, CH), 121.3 (s, CH), 120.6 (s, CH), 120.0 (s, C), 119.7 (s, CH), 109.5 (s, CH), 103.3 (s, CH), 30.6 (s, CH$_3$). **GCMS** (EI, 70 eV) 337 (19) [$C_{19}H_{14}{}^{81}BrN^{\bullet}$]$^+$, 335 (20) $[C_{19}H_{14}{}^{79}BrN^{\bullet}]^+$, 256 (100) $[C_{19}H_{14}N]^+$, 241 (73) $[C_{18}H_{11}N]^+$. **HRMS** (EI+) $[M]^+$ calcd. for $C_{19}H_{14}{}^{79}BrN^+$ 335.0304, found 335.0314. $[M]^+$ calcd. for $C_{19}H_{14}{}^{81}BrN^+$ 337.0284, found 337.0296. $[M\text{-}Br]^+$ calcd. for $C_{19}H_{14}N^+$ 256.1121, found 256.1125. $[M\text{-}Br\text{-}CH_3]^+$ calcd. for $C_{18}H_{11}N^+$ 241.0886, found 241.0891.

Compound 2

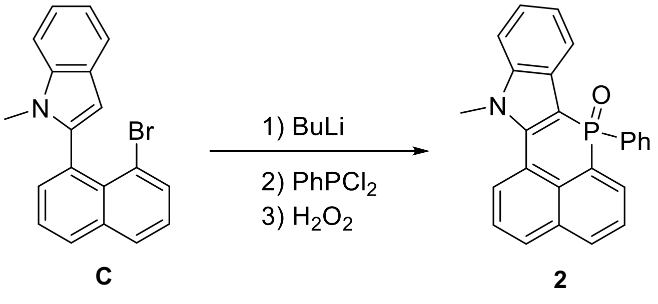

Scheme S2. Synthetic scheme for the preparation of Compound **2**.

Compound **2** was prepared from a modification of a procedure reported earlier.[S1] 88 µL (1 eq, 149 µmol) of ^{t}BuLi 1.7 M in pentane were added to a solution of 2-(8-Bromonaphthalen-1-yl)-1-methyl-1*H*-indole (1 eq, 149 µmol, 50 mg) dissolved in 3 mL of diethyl ether and 1 mL of THF at -78 °C. After 2 min, the lithiated intermediate was reacted with $PhPCl_2$ (1.1 eq, 164 µmol, 29 mg, 22 µL) dissolved in 1 ml of diethyl ether at 0 ºC and the crude mixture was stirred at room temperature for 2 h. After evaporation of the solvent under reduced pressure, the residue was re-dissolved in DCM and two drops of H_2O_2 in 1 mL of H_2O were added at 0 °C. The mixture was stirred for 30 min, quenched with water and the organic layer was separated. The latter was washed three times with water and dried over $MgSO_4$. The solvent was removed and the crude was purified by column chromatography, using alumina and DCM/acetone as eluent mixture (progressively increasing the polarity from pure DCM to DCM/acetone 9.5:0.5). 23 mg of a green solid were obtained (Yield: 40 %). **^{1}H NMR** (600 MHz, in CD_2Cl_2): δ 8.42 (d, *J* = 7.4 Hz, 1H), 8.19 – 8.15 (m, 2H), 8.03 (d, *J* = 8.0 Hz, 1H), 7.77 – 7.66 (m, 5H), 7.52 (d, *J* = 8.3 Hz, 1H), 7.43 – 7.41 (m, 1H), 7.38 – 7.34 (m, 3H), 7.15 (t, *J* = 7.6 Hz, 1H), 4.27 (s, 3H). **^{13}C{^{1}H}, DEPT 135 and ^{13}C{^{1}H}{^{31}P} NMR** (151 MHz, in CD_2Cl_2): δ 142.5 (d, *J* = 15.3 Hz, C), 140.9 (d, *J* = 11.8 Hz, C), 136.6 (d, *J* = 114.4 Hz, C), 133.9 (d, *J* = 6.9 Hz, CH), 133.8 (d, *J* = 9.0 Hz, C), 133.7 (d, *J* = 2.8 Hz, CH), 131.5 (s, CH), 131.5 (d, *J* = 10.4 Hz, CH), 130.8 (s, CH), 129.6 (d, *J* = 101.3 Hz, C), 129.4 (d, *J* = 7.6 Hz, C), 128.6 (d, *J* = 12.5 Hz, CH), 127.8 (d, *J* = 6.9 Hz, C), 126.6 (d, *J* = 12.5 Hz, CH), 126.6 (d, *J* = 1.4 Hz, CH), 126.1 (s, CH), 124.4 (s, CH), 124.2 (d, *J* = 5.5 Hz, C), 122.0 (s, CH), 121.0 (d, *J* = 1.4 Hz, CH), 110.7 (s, CH), 103.8 (d, *J* = 122.8 Hz, C), 35.8 (s, CH_3). **^{31}P{^{1}H} NMR** (243 MHz, in CD_2Cl_2): δ 6.33. **HRMS** (DART+) $[M+H]^+$ calcd. for $C_{25}H_{19}NOP^+$ 380.1199, found 380.1200. Anal. calcd. for $C_{25}H_{18}NOP$: C, 79.14; H, 4.78; N, 3.69, found C, 79.22; H, 4.86; N, 3.74.

3. DFT Calculations

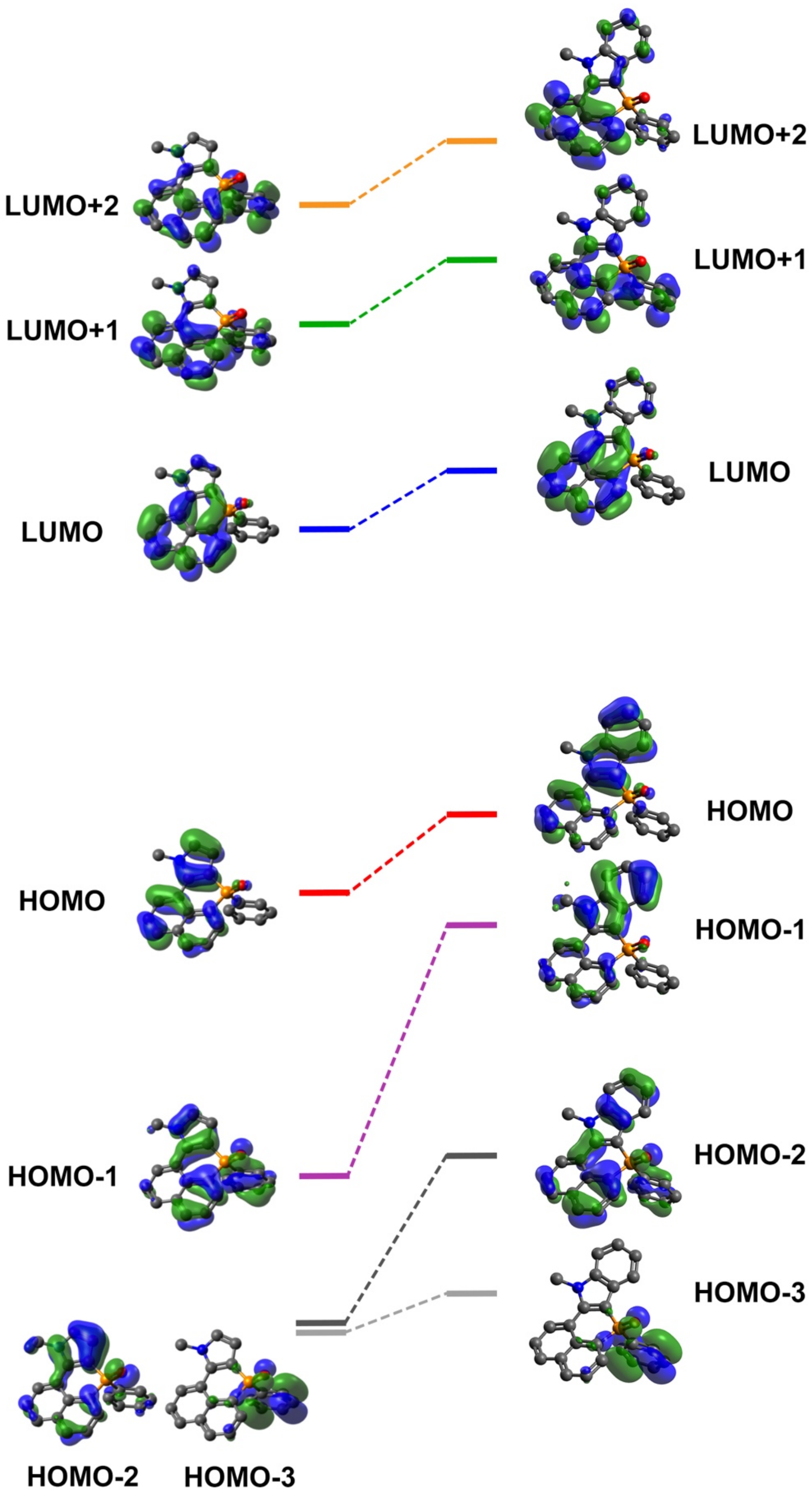

Figure S1. a) Electronic density distribution of **1** (left) and **2** (right) at the B3LYP/6-31+G(d) level of theory. See Table S1 for values.

Table S1. Orbitals' energy obtained by TD-DFT calculations at the B3LYP/6-31+G(d) level of theory.

	Compound 1 (eV)	**Compound 2 (eV)**
LUMO+2	-0.755	-0.526
LUMO+1	-1.006	-0.756
LUMO	-1.985	-1.864
HOMO	-5.722	-5.463
HOMO-1	-6.63	-5.867
HOMO-2	-6.922	-6.452
HOMO-3	-6.971	-6.732
Band GAP	3.737	3.599

Table S2. Photo-induced transitions obtained by TD-DFT calculations at the B3LYP/6-31+G(d) level of theory using dichloromethane as solvent.

Compound 1	**Calc. λ_{max} (nm)**	***f*[a]**
HOMO→LUMO	383.2	0.2332
HOMO-3→LUMO **HOMO→LUMO+1** **HOMO→LUMO+2**	313.3	0.0227
HOMO-3→LUMO **HOMO-2→LUMO** **HOMO-1→LUMO** **HOMO→LUMO+1** **HOMO→LUMO+2**	301.1	0.0228

Compound 2	**Calc. λ_{max} (nm)**	***f*[a]**
HOMO→LUMO	394.1	0.2404
HOMO-1→LUMO	351.8	0.2079
HOMO-3→LUMO **HOMO-2→LUMO** **HOMO-1→LUMO** **HOMO→LUMO+1** **HOMO→LUMO+2**	313.1	0.0484

[a] Oscillator strength

4. Electrochemistry of compound 2

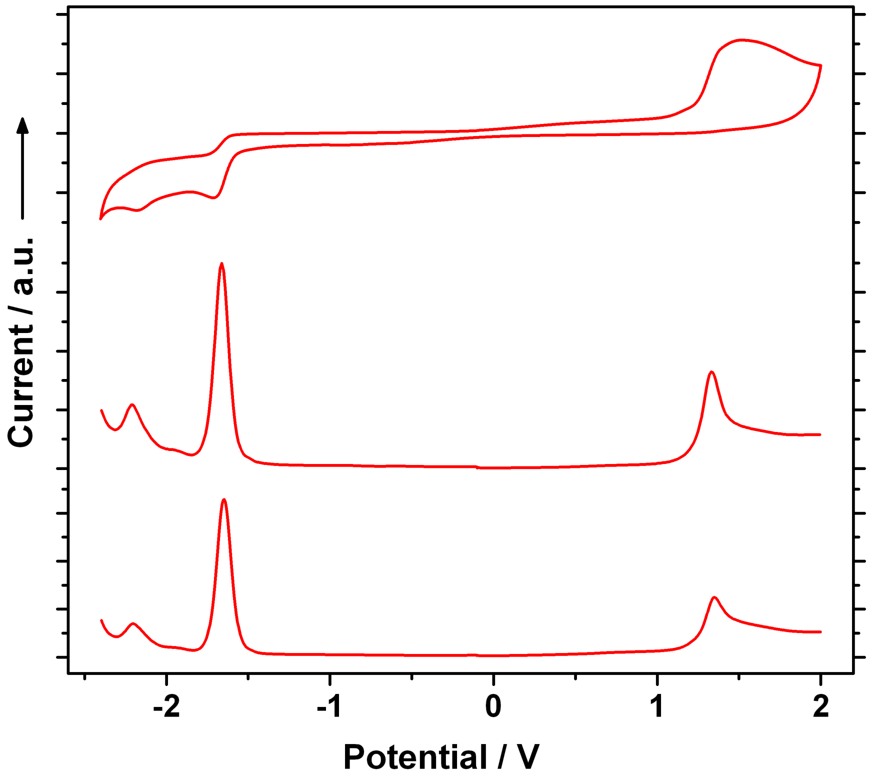

Figure S2. Voltammograms of compound **2** obtained from cyclic voltammetry (upper graph), differential pulse voltammetry (middle graph) and square wave voltammetry (bottom graph). Note that the oxidation process in differential pulse and square wave voltammetries appears as a broad band; i.e. the maximum possesses a tail towards higher positive potentials.

5. Steady state spectroscopy of 1 and 2

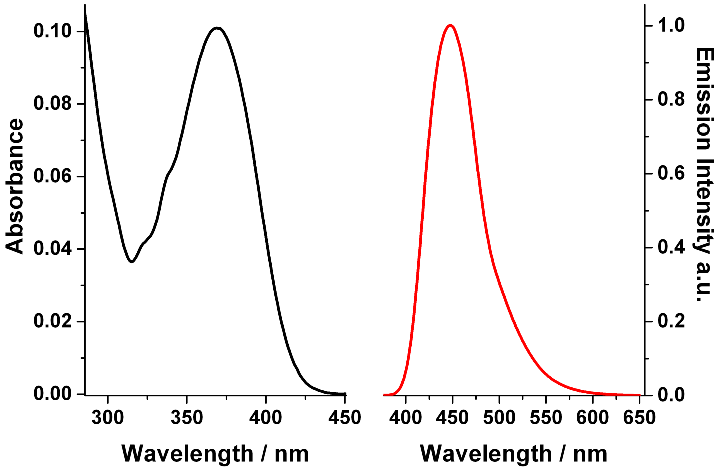

Figure S3. Absorption and emission spectra of **1** obtained from DCM solutions.

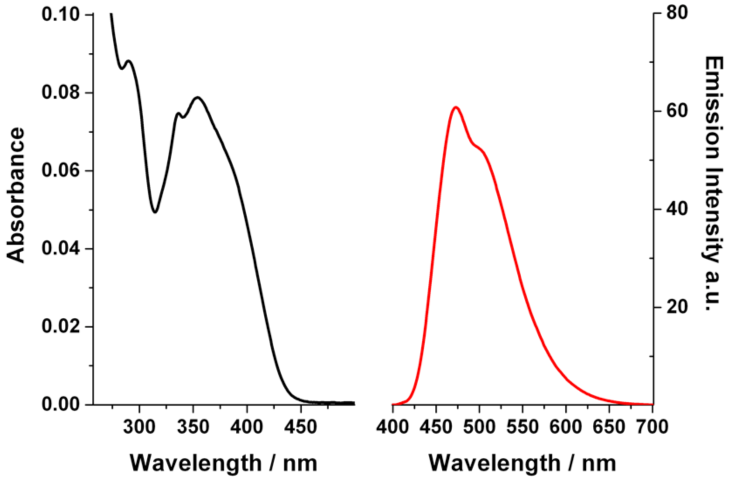

Figure S4. Absorption and emission spectra of **2** obtained from DCM solutions.

Table S3. Summary of the photophysical properties of compounds **1** and **2**.

Compound	λ_{abs} (nm)[a]	λ_{em} (nm)[b]	τ1 (ns)[c]	Φ[d]	Kr (s^{-1})[f]	Knr (s^{-1})[g]
1[e]	367	450	9.9	0.8	8.08E+07	2.02E+07
2	355	473	4.6	0.15	3.26E+07	1.85E+08

[a] Absorption maxima recorded from DCM solutions. [b] Emission maxima recorded from DCM solutions. [c] Fluorescence lifetimes. [d] Fluorescence quantum yields relative to quinine sulfate in 0.1M H_2SO_4, $\Phi = 0.54$. [e] Data previously reported in ref. S1. [e] Radiative constant. [f] Non-radiative constant.

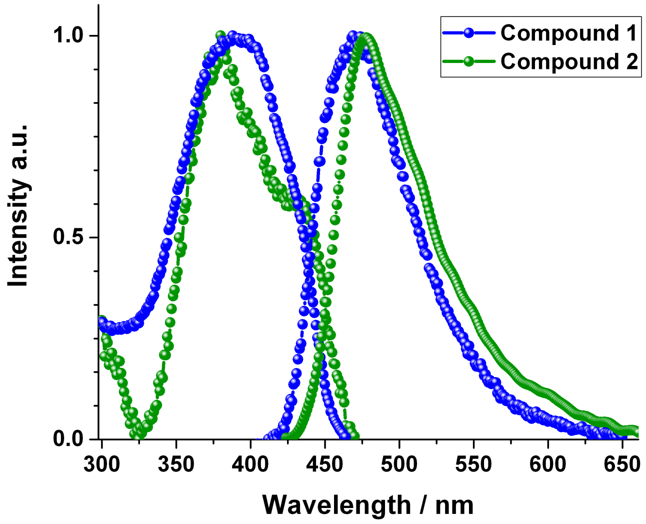

Figure S5. Solid-state excitation and emission spectra of **1** and **2**.

6. Thermogravimetric analyses (TGA)

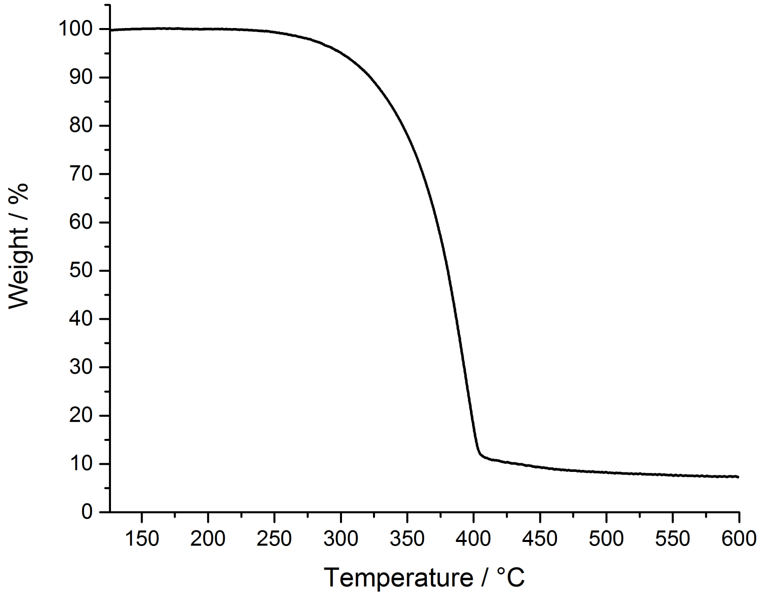

Figure S6. Thermal decomposition under inert conditions of compound **1**.

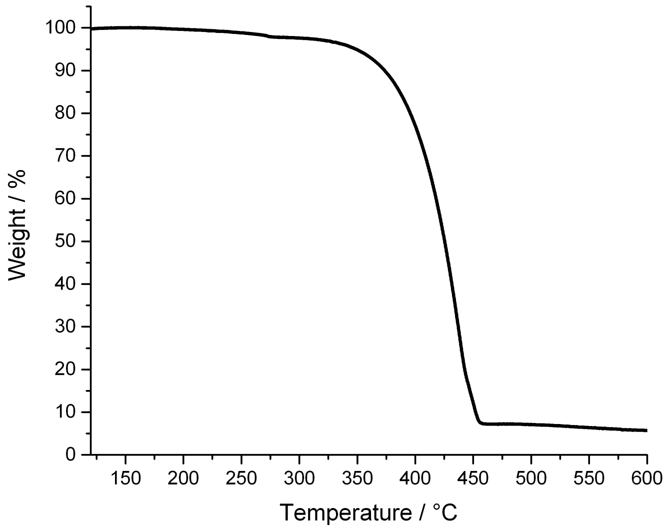

Figure S7. Thermal decomposition under inert conditions of compound **2**.

7. Device Optimization

For the optimization of the devices based on compound **1** the fabrication parameters were varied according to Table S4. The solvents toluene, *ortho*-dichlorobenzene and dichloromethane were investigated at different concentrations and different spin speeds to achieve varying thicknesses and to influence film morphology. Furthermore a host/guest-system was analyzed using bis[2-(diphenylphosphino)phenyl] ether oxide (**DPEPO**) as host material (HOMO = 6.1 eV, LUMO = 2.0 eV). The ratio M1:DPEPO was varied according to Table S4. The best performing devices were fabricated using a toluene solution without the DPEPO host at a concentration of 5 g/l. The spin speed was 500 rpm which resulted in a thickness of 48 ±7 nm for the emissive layer.

Table S4. Summary of the different device parameters investigated for the optimization of devices using compound **1**.

Solution	Thickness (nm)	Max. Luminance (cd m^{-2})	Turn-on voltage (V)	Max. Efficiency (cd A^{-1})	Max. Efficacy (lm W^{-1})
Toluene, 10 g l^{-1}	70 ±11	13 ±15	10.7 ±1.6	0.052 ±0.068	0.014 ±0.019
Toluene, 10 g l^{-1}	63 ±8	15 ±18	8.8 ±0.1	0.11 ±0.145	0.035 ±0.046
Toluene, 5 g l^{-1}	48 ±7	694 ±13	5.3 ±0.1	0.1 ±11	0.133 ±0.01
Toluene, 2 g l^{-1}	18 ±11	250 ±19	5.2 ±0.1	0.053 ±0.005	0.019 ±0.01
oDCB, 10 g l^{-1}	91 ±4	50 ±24	5.9 ±0.7	0.063 ±0.045	0.025 ±0.015
oDCB, 10 g l^{-1}	86 ±11	49 ±3	6.0 ±1.2	0.023 ±0.023	0.01 ±0.011
oDCB, 10 g l^{-1}	73 ±8	82 ±39	4.7 ±0.3	0.04 ±0.017	0.02 ±0.007
oDCB, 5 g l^{-1}	31 ±2	49 ±20	4.2 ±0.1	0.018 ±0.004	0.009 ±0.003
oDCB, 5 g l^{-1}, filtered	33 ±2	36 ±16	4.3 ±1.0	0.016 ±0.004	0.009 ±0.002
DCM, 10 g l^{-1}	77 ±17	45 ±5	9.7 ±1	0.053 ±0.004	0.003 ±0.001
DCM, 10 g l^{-1}, M1:DPEPO	76 ±20	-	-	-	-
DCM, 10 g l^{-1}, M1:DPEPO	132 ±10	-	-	-	-
DCM, 10 g l^{-1}, M1:DPEPO	102 ±30	-	-	-	-
DCM, 10 g l^{-1}, M1:DPEPO	84 ±13	26 ±2	14.5 ±0.06	0.032 ±0.068	0.059 ±0.013
DCM, 10 g l^{-1}, M1:DPEPO 1:1	112 ±31	-	-	-	-

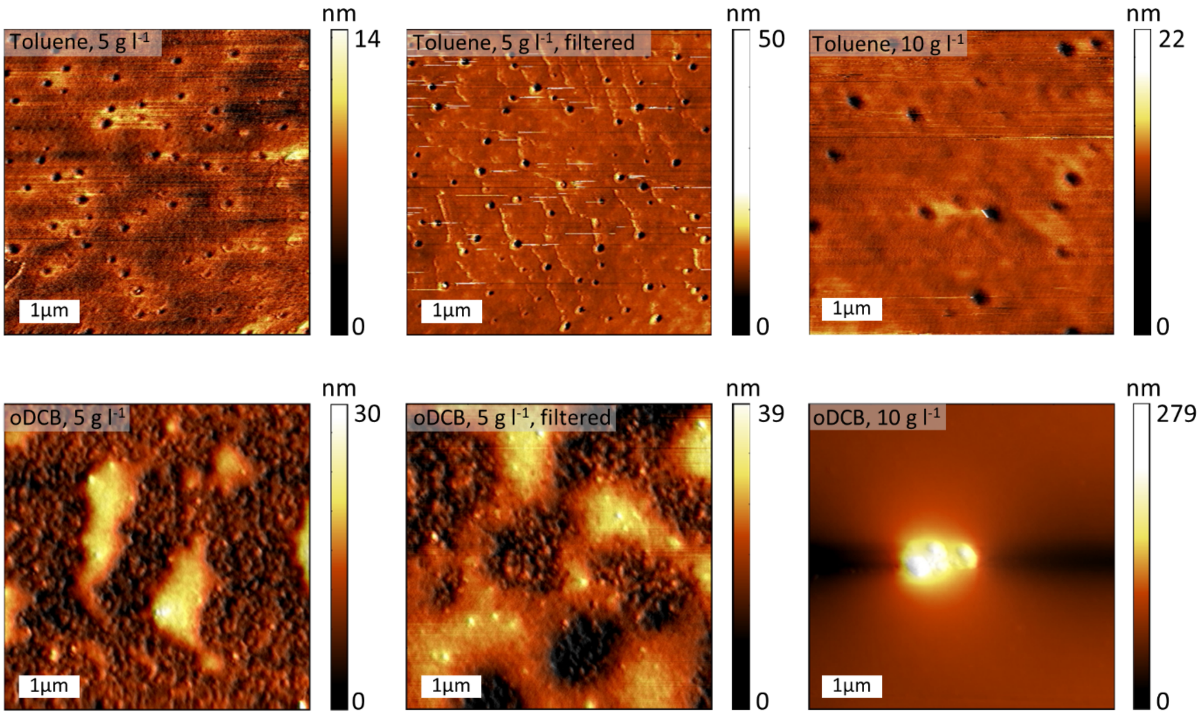

Figure S8. AFM images of the emissive layers, spin coated from different solutions.
(Upper images) AFM pictures of spin coated samples from toluene solutions. Holes in the emissive layers are observed, which contributed to an inhomogeneous light emission. Neither filtering the solution nor increasing the concentration to increase film thickness could significantly improve the morphology. (Bottom images) AFM pictures of spin coated samples from *ortho*-dichlorobenzene solutions. Totally closed films are observed, however, agglomerates in the emissive layer are present, which were responsible for the lower performance. All images are recorded at a resolution of 512 × 512 nm for 5 × 5 µm with a DME DualScope 95-50 atomic force microscope.

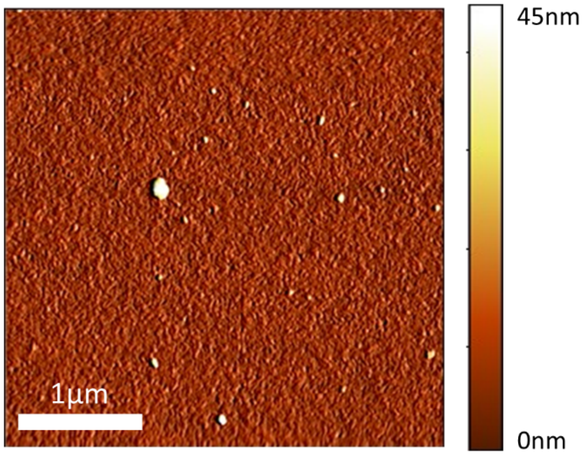

Figure S9. AFM of spin-coated compound **2** PEDOT:PSS/ITO/glass.

8. NMR Data

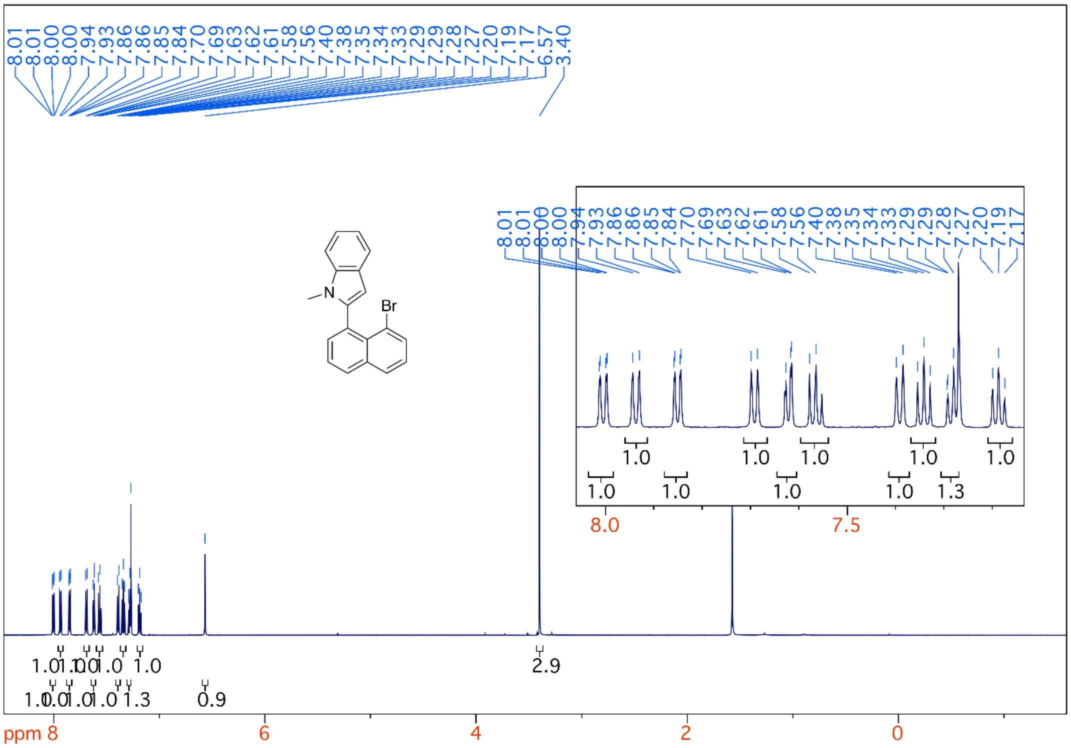

Figure S10. ${}^{1}H$ NMR (600 MHz, $CDCl_3$) spectrum of 2-(8-Bromonaphthalen-1-yl)-1-methyl-1*H*-indole

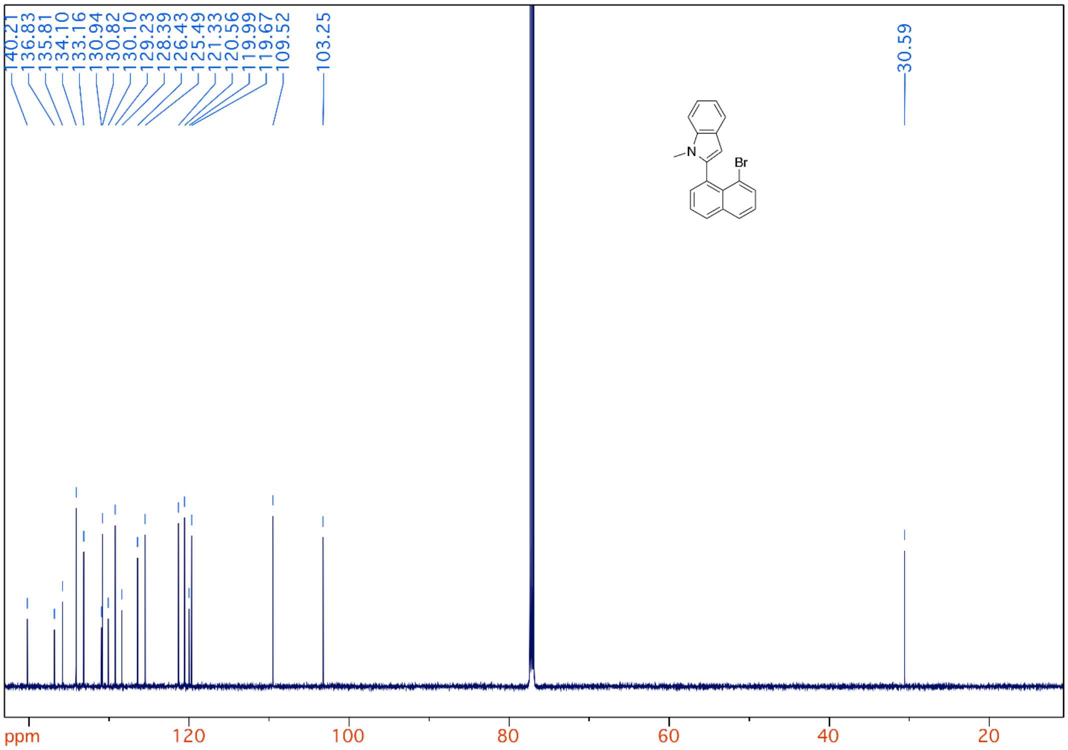

Figure S11. ${}^{13}C\{{}^{1}H\}$ NMR (151 MHz, in $CDCl_3$) spectrum of 2-(8-Bromonaphthalen-1-yl)-1-methyl-1*H*-indole

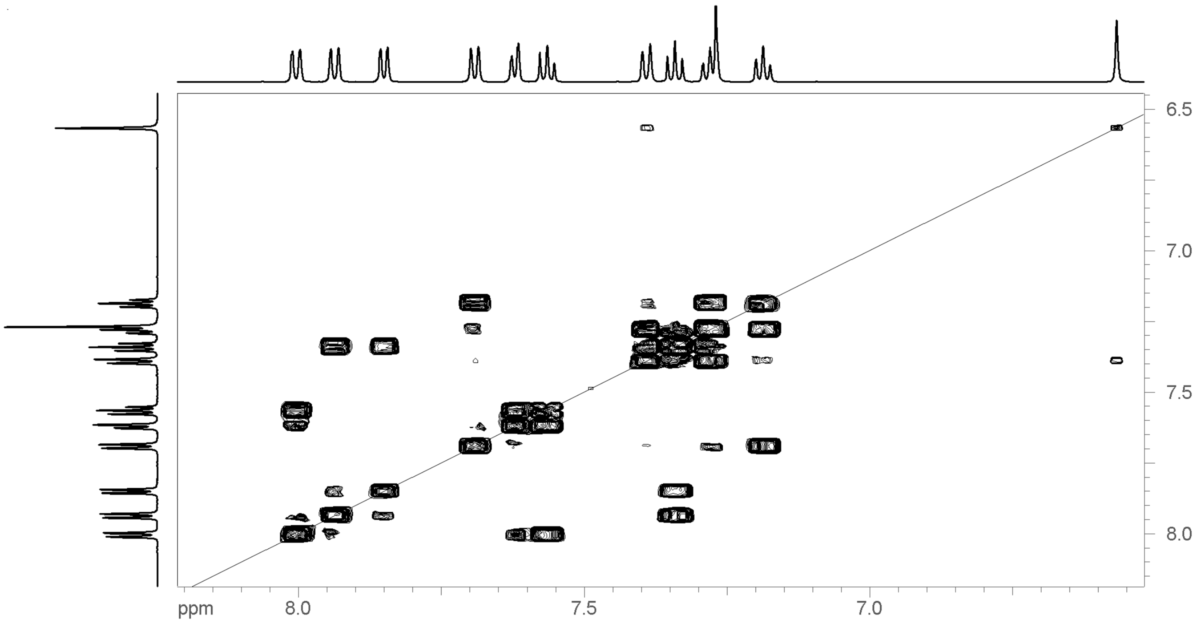

Figure S12. ^{1}H-^{1}H COSY NMR (400 MHz, in $CDCl_3$) spectrum of 2-(8-Bromonaphthalen-1-yl)-1-methyl-1*H*-indole

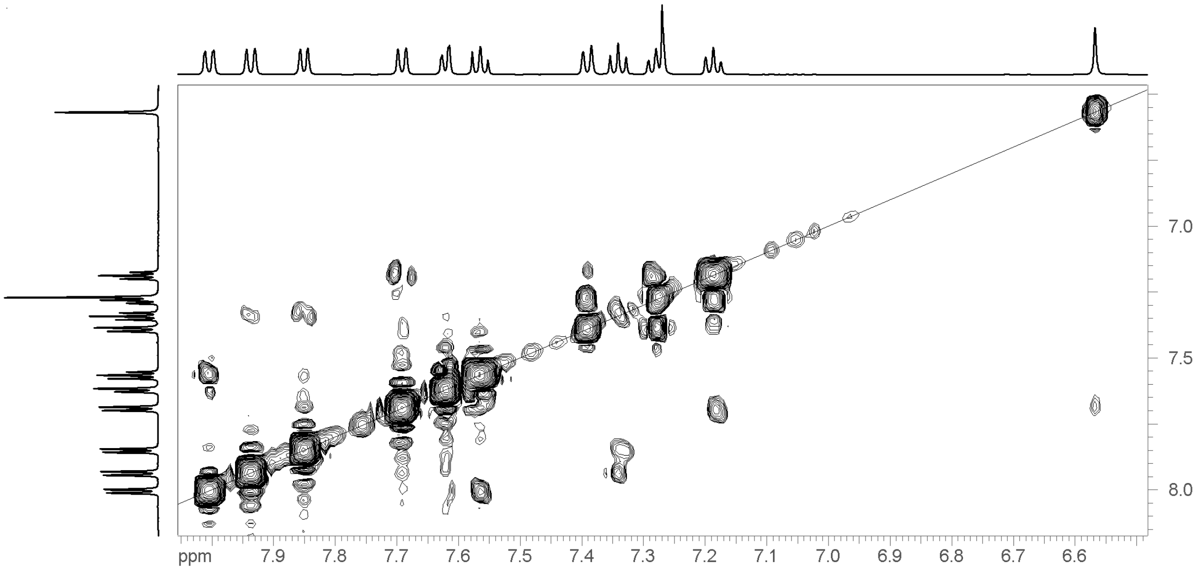

Figure S13. ROESY NMR (400 MHz, in $CDCl_3$) spectrum of 2-(8-Bromonaphthalen-1-yl)-1-methyl-1*H*-indole

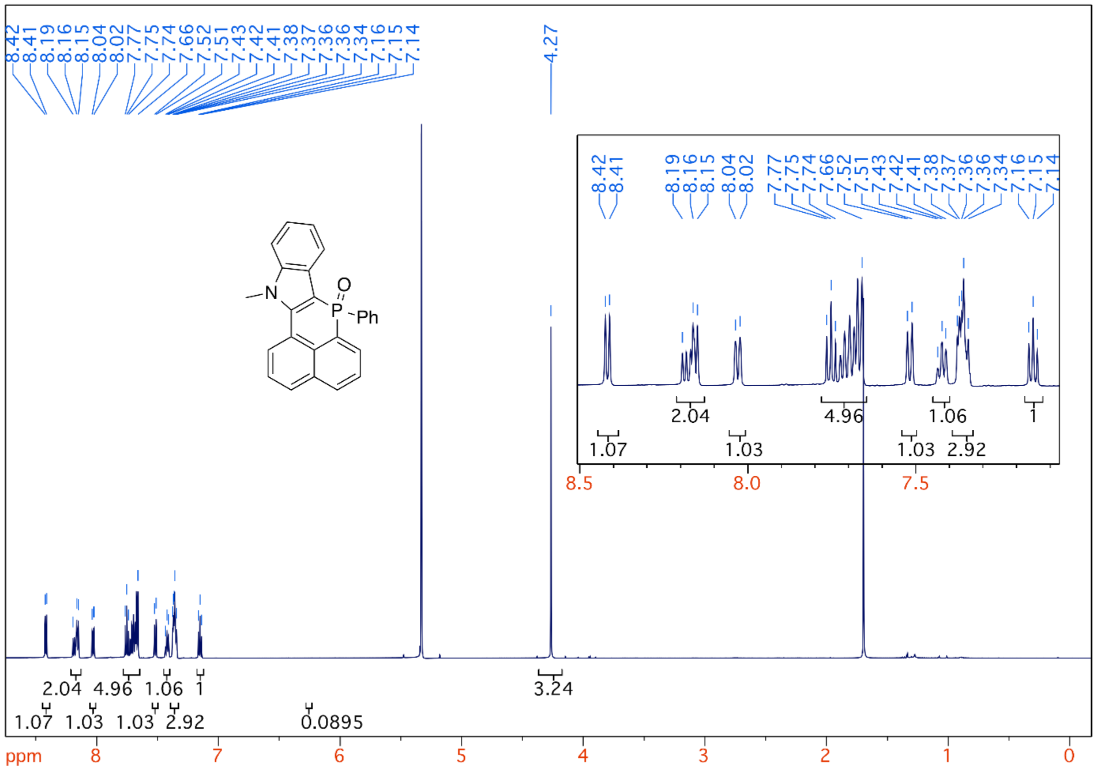

Figure S14. ^{1}H NMR (600 MHz, CD_2Cl_2) spectrum of Compound **2**

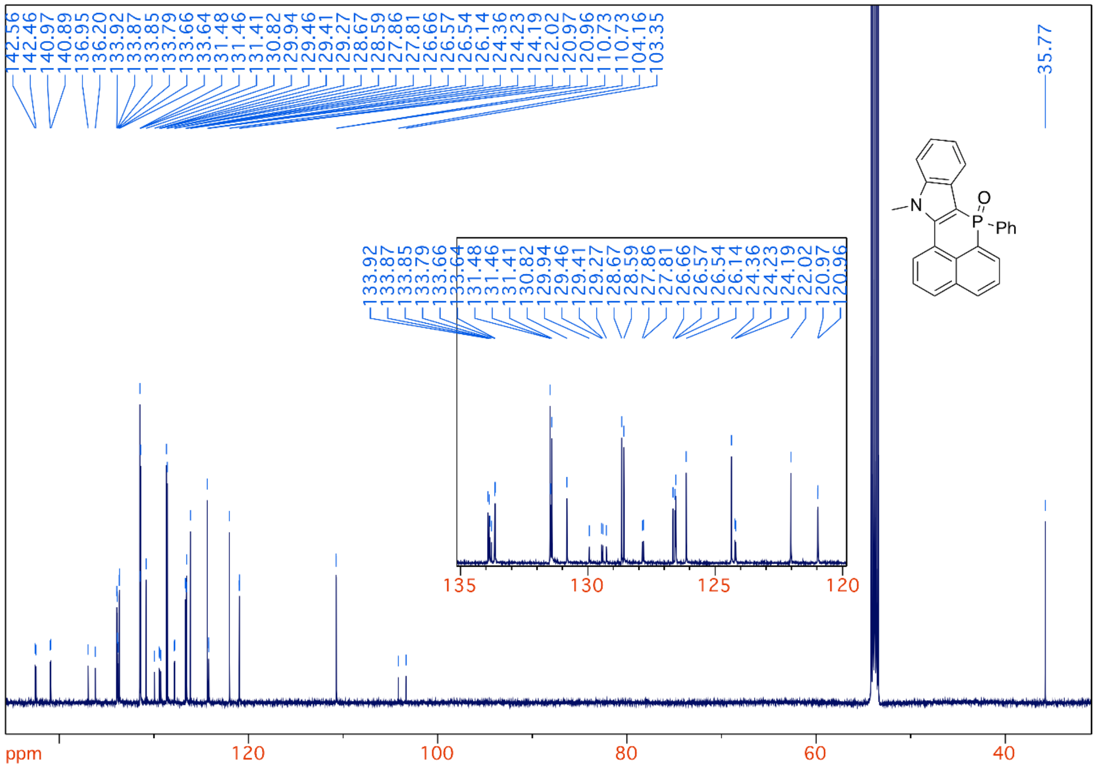

Figure S15. $^{13}C\{^1H\}$ NMR (151 MHz, in CD_2Cl_2) spectrum of Compound **2**

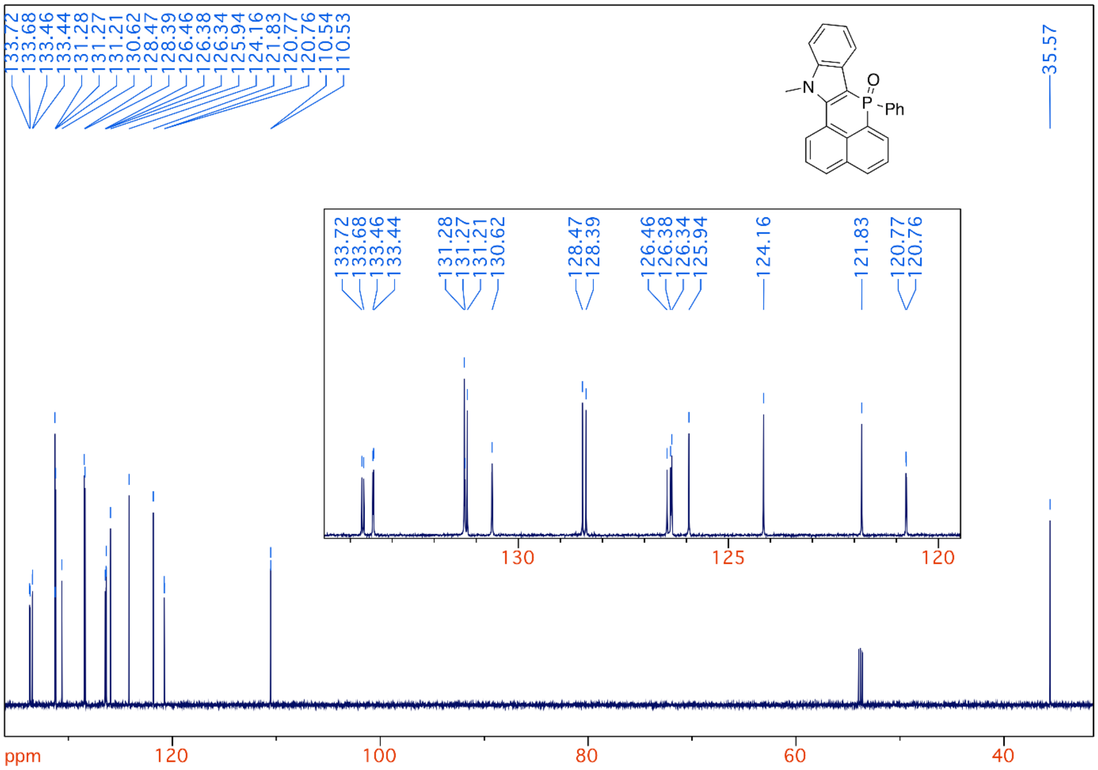

Figure S16. ^{13}C DEPT 135 (151 MHz, in CD_2Cl_2) spectrum of Compound **2**

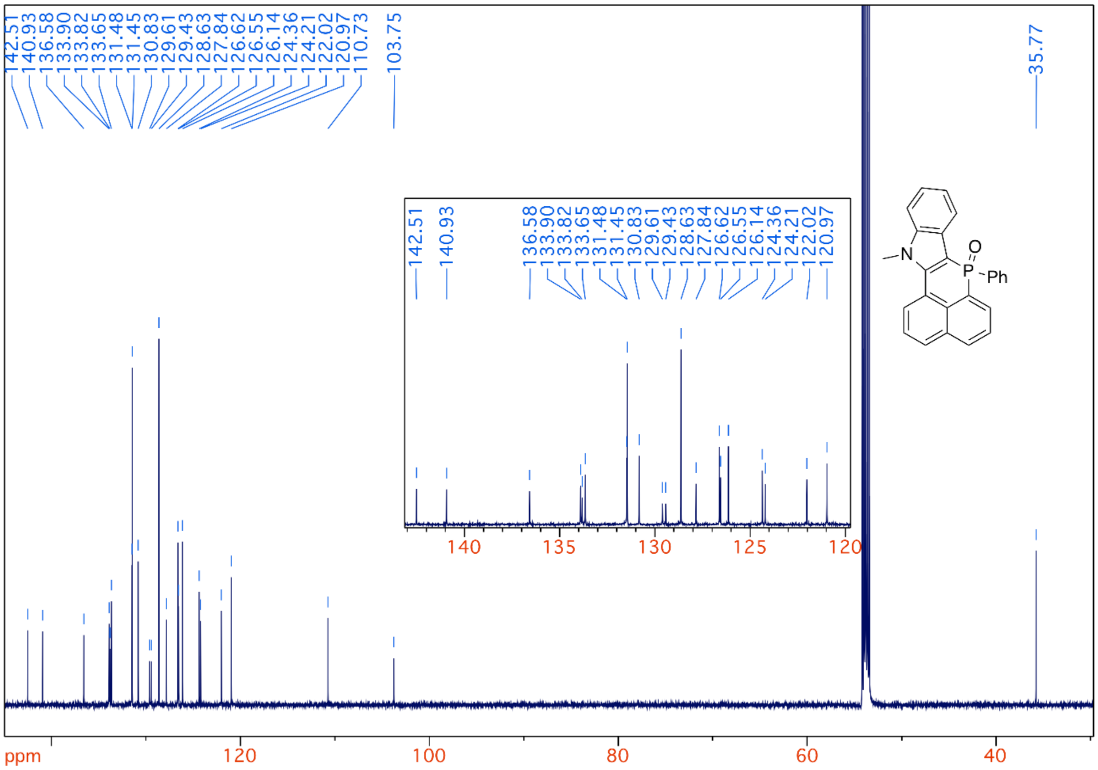

Figure S17. $^{13}C\{^1H\}\{^{31}P\}$ NMR (151 MHz, in CD_2Cl_2) spectrum of compound **2**

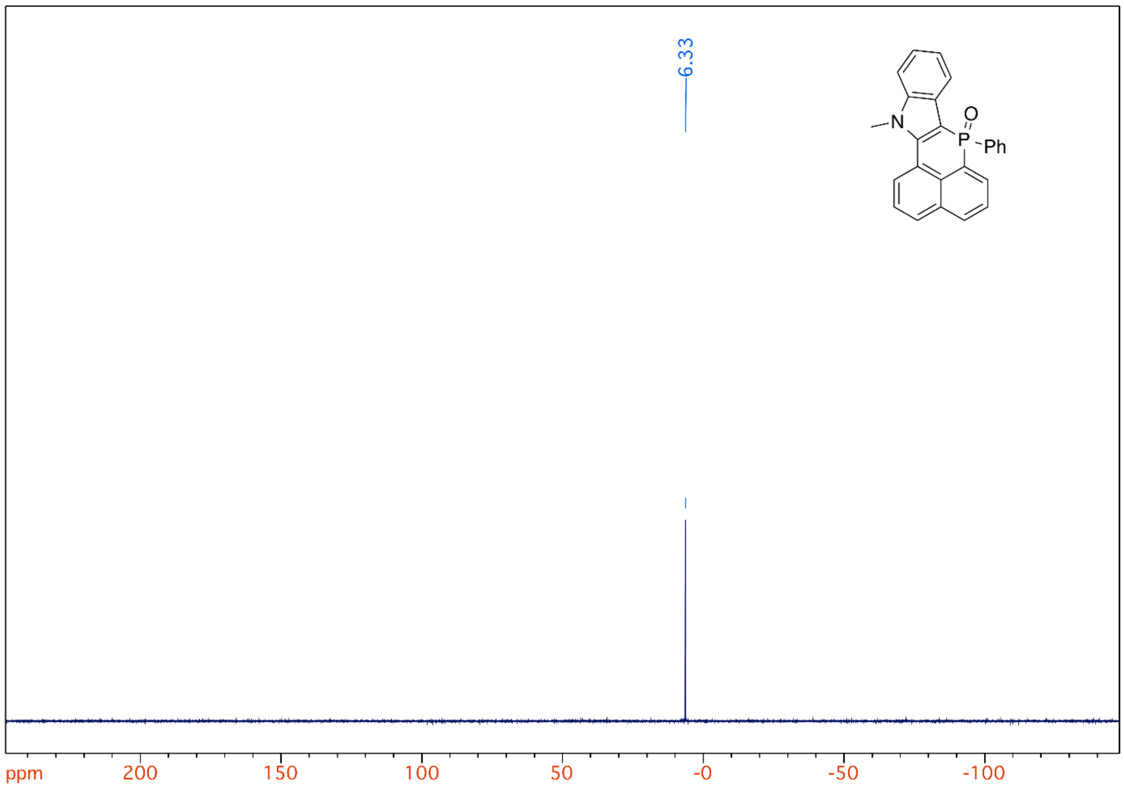

Figure S18. $^{31}P\{^1H\}$ NMR (242 MHz, in CD_2Cl_2) spectrum of compound **2**

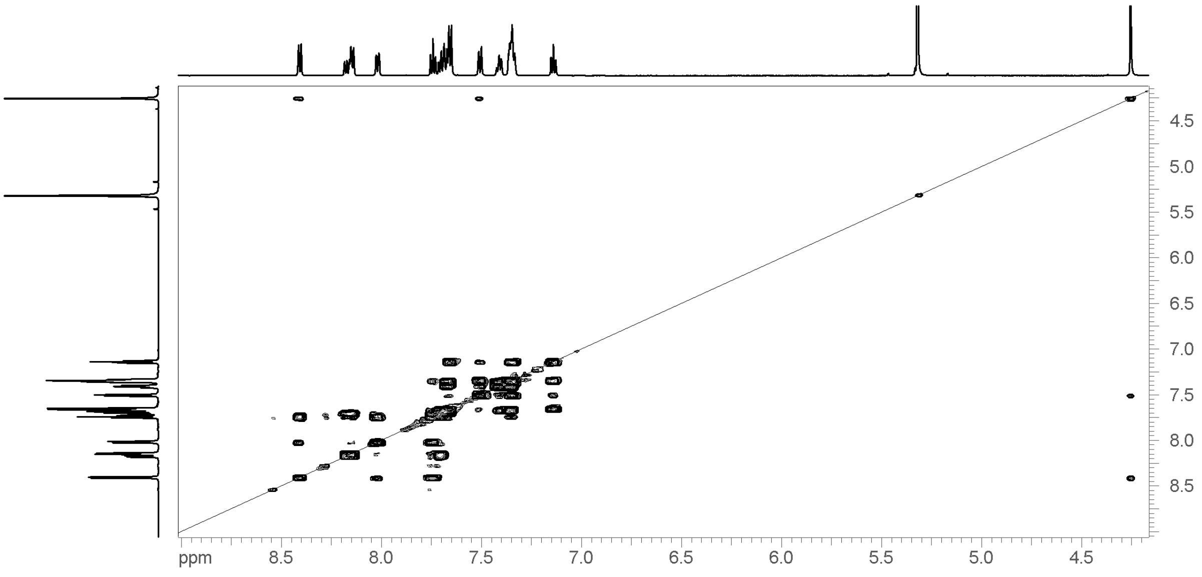

Figure S19. ^1H-^1H COSY NMR (400 MHz, in CD_2Cl_2) spectrum of Compound **2**

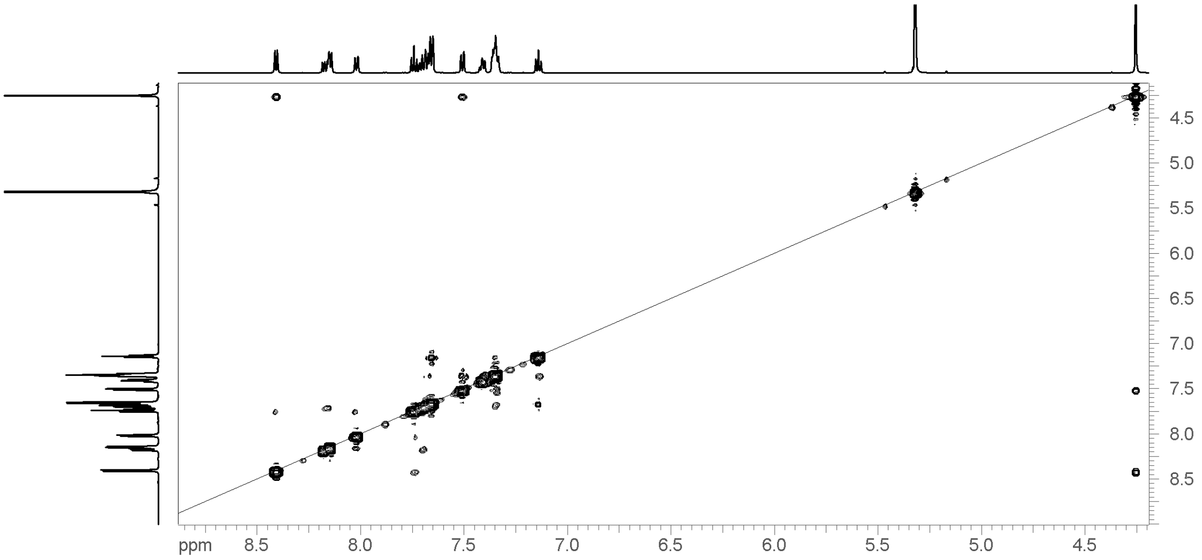

Figure S20. ROESY NMR (400 MHz, in CD_2Cl_2) spectrum of Compound **2**

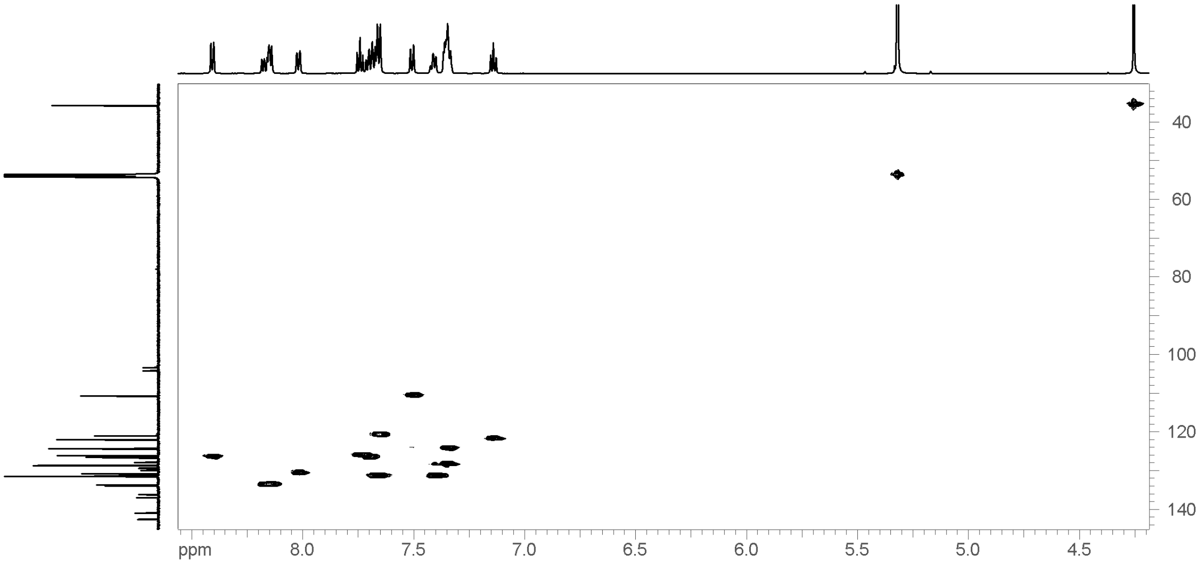

Figure S21. HSQC-DEPT NMR (400 MHz, in CD_2Cl_2) spectrum of Compound **2**

9. Literature

S1. Romero-Nieto, C.; López-Andarias, A.; Egler-Lucas, C.; Gebert, F.; Neus, J.-P.; O. Pilgram, *Angew. Chem. Int. Ed.* **2015**, *54*, 15872-15875.

S2. Full reference for the theoretical calculations: Gaussian 03, Revision E.01, Frisch, M. J.; Trucks, G. W.; Schlegel, H. B.; Scuseria, G. E.; Robb, M. A.; Cheeseman, J. R.; Montgomery, J. A.; Vreven, Jr. T.; Kudin, K. N.; Burant, J. C.; Millam, J. M.; Iyengar, S. S.; Tomasi, J.; Barone, V.; Mennucci, B.; Cossi, M.; Scalmani, G.; Rega, N.; Petersson, G. A.; Nakatsuji, H.; Hada, M.; Ehara, M.; Toyota, K.; Fukuda, R.; Hasegawa, J.; Ishida, M.; Nakajima, T.; Honda, Y.; Kitao, O.; Nakai, H.; Klene, M.; Li, X.; Knox, J. E.; Hratchian, H. P.; Cross, J. B.; Bakken, V.; Adamo, C.; Jaramillo, J.; Gomperts, R.; Stratmann, R. E.; Yazyev, O.; Austin, A. J.; Cammi, R.; Pomelli, C.; Ochterski, J. W.; Ayala, P. Y.; Morokuma, K.; Voth, G. A.; Salvador, P.; Dannenberg, J. J.; Zakrzewski, V. G.; Dapprich, S.; Daniels, A. D.; Strain, M. C.; Farkas, O.; Malick, D. K.; Rabuck, A. D.; Raghavachari, K.; Foresman, J. B.; Ortiz, J. V.; Cui, Q.; Baboul, A. G.; Clifford, S.; Cioslowski, J.; Stefanov, B. B.; Liu, G.; Liashenko, A.; Piskorz, P.; Komaromi, I.; Martin, R. L.; Fox, D. J.; Keith, T.; Al-Laham, M. A.; Peng, C. Y.; Nanayakkara, A.; Challacombe, M.; Gill, P. M. W.; Johnson, B.; Chen, W.; Wong, M.W.; Gonzalez, C.; Pople, J. A. Gaussian Inc., Wallingford, CT, USA 2007.